Spectrograph

Document Number ..... *No Number*
Revision: ..... Version 1.0
Date ..... April 27th 2020
Status ..... Under Review

Prepared By	Name	A. Tozzi	Signature	
	Organisation	INAF-Arcetri	Date	April 27th 2020
	Organisation		Date	

TABLE OF CONTENT

LIST OF FIGURES

1 DESCRIPTION OF A SPECTROGRAPH.

In this chapter a review of the main parameters and formulas of a spectrograph are described. They are useful because these quantities are used in the Excel HR-MOS Calculator (ExMoCa).

1.1 Main parameters and formulas

On the focal plane of a telescope with a diameter of D_{tel} it is placed a rectangular slit: it is the real input of the spectrograph that forms the dispersed image of this object on the detector.

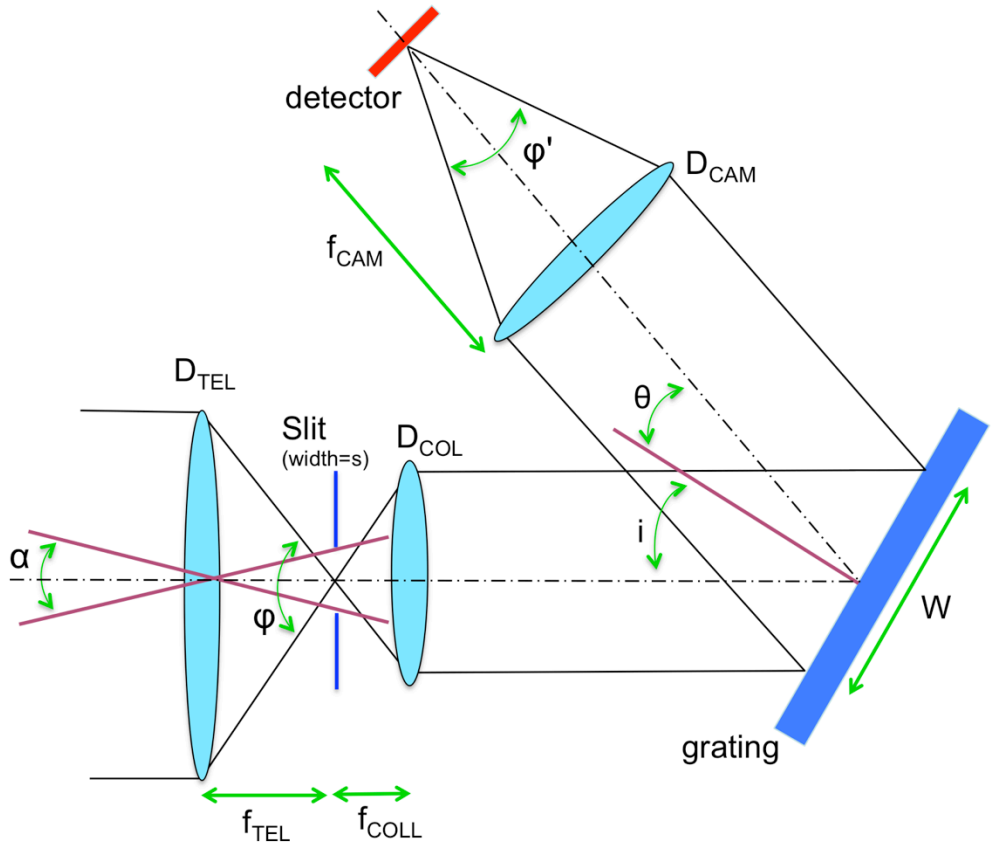

Figure 1 Schema of a direct fed spectrograph. In green the main quantities.

The aperture of the slit corresponds to a certain angular aperture α in the sky (typical values are in the order of 0.5”- 2”). The function of the slit is to select, in the field of view of the telescope, the sources of which to obtain the desiderd spectrum.

Beyond the slit is the collimator, an optical system that serves to produce a collimated beam of D_{coll} diameter, that is, parallel rays that reach the grating. φ is the opening angle

of the light beam that hits the collimator. The normal to the grating surface is inclined by an angle of incidence prelist with respect to the direction of arrival of the collimated beam and W is the linear dimension of the grating area illuminated by the incident beam. As the angle changes, the spectrum is generated. The light then propagates towards the camera lens of diameter D_{cam} and focal length f_{cam}, which focuses the spectrum on the detector. φ' is the beam opening angle focused by the camera lens.

The grating is an optical device realized by grooves and how it is made in really it is not important for the moment: it can be a reflected gratin gas in figure, buti t can be a transmission grating. The only parameter that is important, is the density if the grooves, ρ, expressed in lines for millimetre.

The main grating equations, derived from the Fraunhofer interference, are:

$$\sin i + \sin \vartheta = \rho m \lambda$$

$$\frac{\Delta\lambda}{\Delta\vartheta} = \frac{\cos\vartheta}{\rho m}$$

$$\frac{\Delta\lambda}{\Delta x} = \frac{\cos\vartheta}{\rho m\, f_{CAM}}$$

$$R^* = \frac{\lambda}{\Delta\lambda} = \rho m\, W$$

where R* is the theoric resolving power for a slit of thickness zero, W is the length of the grating, the coordinate x is the detector spectral direction (y is the spatial direction), m is the order of the spectrum.

We now derive the expression for the effective resolving power R, which as we will see depends not only on the characteristics of the grating, but also on other factors, including the real width of the slit.
Let s be the linear width of the slit and s′ the linear width of its image on the detector. We apply the Lagrange invariance of the optical systems:

$$n\Omega A = constant$$

where Ω is the solid angle of the incoming beam on the surface A in a material of refraction index equal to n.

So applying the Lagrange invariance to the slit width, that is in air as the detector,

$$s\varphi = s'\,\varphi'$$

we obtain

$$s\frac{D_{coll}}{f_{coll}} = s'\frac{D_{cam}}{f_{cam}} \qquad (1)$$

$$s' = s\frac{D_{coll}}{f_{coll}}\frac{f_{cam}}{D_{cam}} = s\frac{F_{cam}}{F_{coll}}$$

where with capital letter F we mean the f-numbe, sometimes expressed as f/#, of the beam (f/# = focal length / diameter). The last equation means that the dimension of the slit on the detector is related only to the f/numbers of the camera lens and the collimator.

Now we can evaluate the resolving power:

$$\Delta\lambda = \frac{\Delta\lambda}{\Delta x}s' = \left(\frac{\cos\vartheta}{\rho m\, f_{cam}}\right)\left(s\frac{D_{coll}}{f_{coll}}\frac{f_{cam}}{D_{cam}}\right) = \frac{s\cos\vartheta}{\rho m\, D_{cam}\, F_{coll}}$$

But the illuminated zone of the grating is W that is a linear dimension equal to

$$W = \frac{D_{cam}}{\cos\vartheta}$$

and so we find that

$$\Delta\lambda = \frac{s}{\rho m\, W\, F_{coll}}$$

And the Real Resolving Power (RRP) is finally:

$$R = \frac{\lambda}{\Delta\lambda} = \rho m W\, \frac{F_{coll}\,\lambda}{s} = R^*\frac{F_{coll}\,\lambda}{s}$$

The real resolving power R of the spectrograph is not depending to the camera characteristic!

It is convenient to rewrite R in terms of sky angle, as usually done in astronomy: the aperture of the slit is $\alpha = {}^{s}/_{f_{tel}}$ where α is expressed in radiant and it is the real width of the scientific object under study. In an ideal and directly fed configuration we have $F_{tel} = F_{coll}$ that it means the f-numbers of the collimator if the same of the telescope, but this is not completely true both in the direct fed and fiber fed case. In a direct fed case the f number of the collimator is done lower that the telescope (Collimator is “faster “ than the telecope) to be sure to collect the light coming from the scientific object taking into account the seeing angle and the defects of the real prelist optical system. In a fiber fed spectrograph the Focal Ratio Degradation changes the apparent f-number of the beam.

With these notes we make the preliminary assumption that:

$$F_{tel} = F_{coll} \rightarrow \frac{f_{tel}}{D_{tel}} = \frac{f_{coll}}{D_{coll}}$$

and finally

$$R = R^*\frac{F_{coll}\,\lambda}{s} = R^*\frac{F_{coll}\,\lambda}{\alpha\, F_{coll} D_{tel}} \Rightarrow R = R^*\frac{\lambda}{\alpha\, D_{tel}}$$

Now we can evaluate an important relation between dispersion and resolution.

We have seen that the resolution for a spectrograph grating directly fed is

$$R = R^* \frac{\lambda}{\alpha\, D_{tel}} = \rho m W \frac{\lambda}{\alpha\, D_{tel}} = \rho m \frac{D_{cam}}{\cos\vartheta} \frac{\lambda}{\alpha\, D_{tel}}$$

But the angular dispersion of the grating defined as ${\Delta\lambda}/{\Delta\vartheta}$ is

$$\frac{\Delta\lambda}{\Delta\vartheta} = \frac{\cos\vartheta}{\rho m}$$

So the resolution R can be expressed as

$$R = \frac{\lambda}{\Delta\lambda} = \left(\frac{D_{cam}}{D_{tel}}\right) \frac{\lambda}{\alpha\left(\frac{\Delta\lambda}{\Delta\vartheta}\right)}$$

$$\Delta\lambda = \left(\frac{D_{tel}}{D_{cam}}\right) \alpha \frac{\Delta\lambda}{\Delta\vartheta}$$

These formulas say that in case of high resolution spectrograph, that it means ${\Delta\lambda}/{\Delta\vartheta} \to 0$, we can have not only high resolution, that it means $R \to \infty$ and $\Delta\lambda \to 0$, but low resolution, for example increasing the slit width.

Vice versa is not true: in case of low dispersion, that it means ${\Delta\lambda}/{\Delta\vartheta} \gg 0$, it is impossible to have high resolution.

The analysed system and the equations derived are mainly good for a fiber fed spectrograph, too.

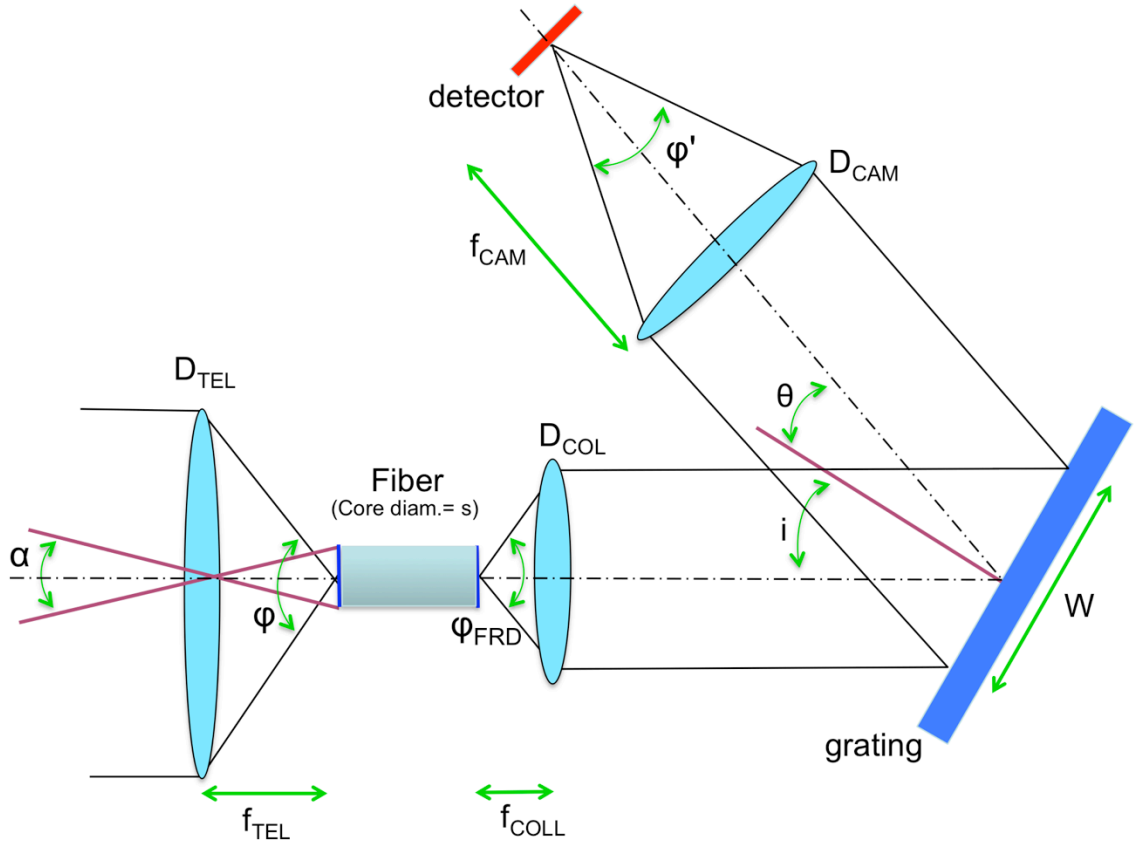

Figure 2 spectrograph fiber fed

The main difference is due to the fiber Focal Ratio Degradation that changes the working f/number of the output beam: the input termination of the fiber is not placed in the telescope focus, this because using fiber it is important to illuminate the surface of the fiber core using a beam with the exact Numerical Aperture of the fiber, that is:

$$input\ beam\ Numerical\ Aperture = \sin\frac{\varphi}{2} = \frac{1}{2\,fnumber}$$

So an auxiliary optics is need to match the correct illumination f/number of the fiber that, let say is something around 3.10. This auxiliary optics deosn't change the equations, because of the Lagrange invariance that is always $D_{tel}\alpha$.

What is changing is the angle of the illuminating beam of the collimator, that is not the same of the telescope: this angle is the f-number of the fiber that it is not exactly the same value of the incoming one, because of the FRD effect. The collimator simply sees a beam having an f-number slightly different with respect the one used for the fiber input :

$$\varphi_{FRD} \cong \varphi_{fiber\ in} \neq \varphi_{telescope}$$

1.2 spectrographs: a real case MOONS

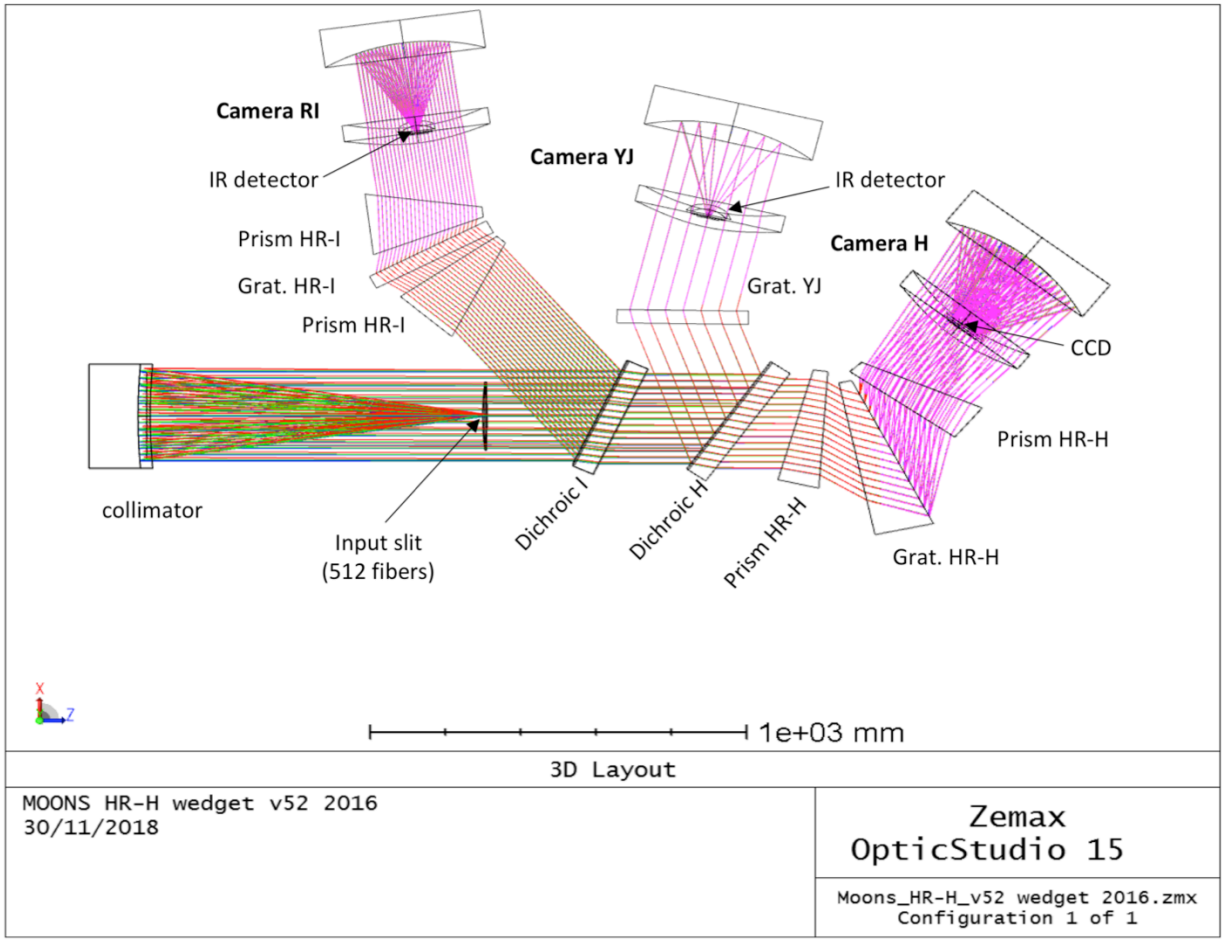

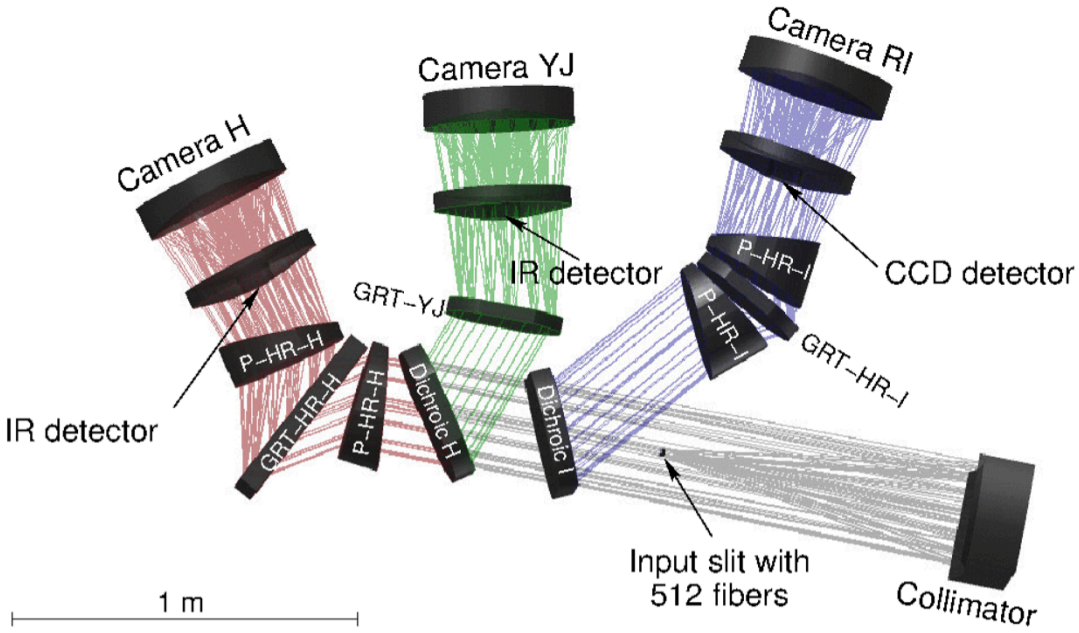

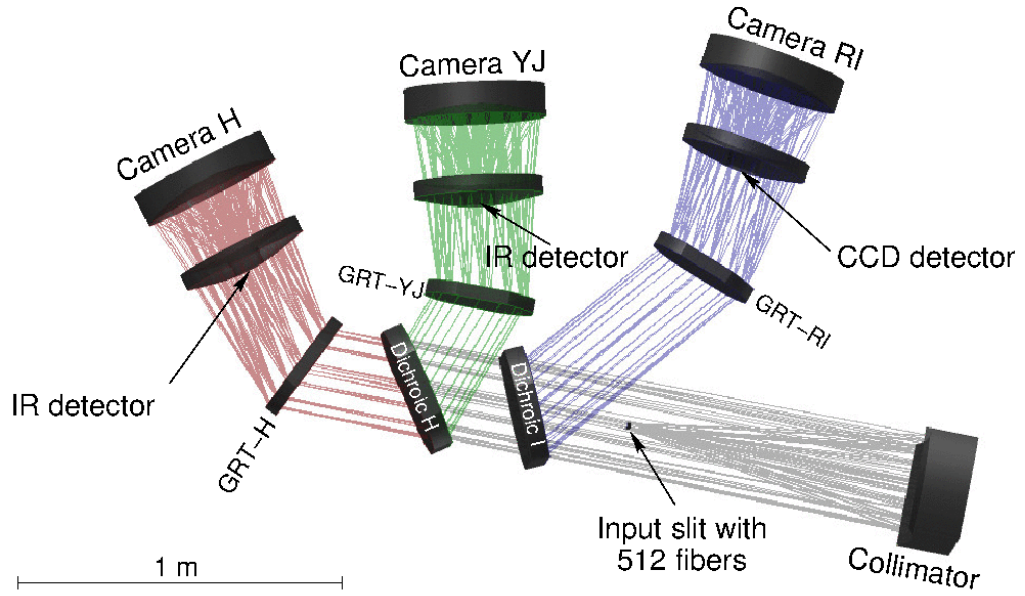

1.3 spectrographs: Blaze angle

In the previous chapter we have seen which are the main quantities involved into the design of a spectrograph. Unfortunately the maximum of light intensity produced by a grating, also called the maximum of blaze, occurs at θ = 0, ie m = 0, where however there is no dispersion and It is therefore necessary that m ≠ 0 for a spectrum to form. Since, however, the intensity of light is modulated by the diffraction figure of the single stretch, the spectrum is already weak at m = 1 and it becomes weaker and weaker as the order grows. So you have to somehow move the blaze maximum to higher orders. This can be

achieved by working the grating sections so that they form an angle δ with the grating plane. This angle is known as the blaze angle.

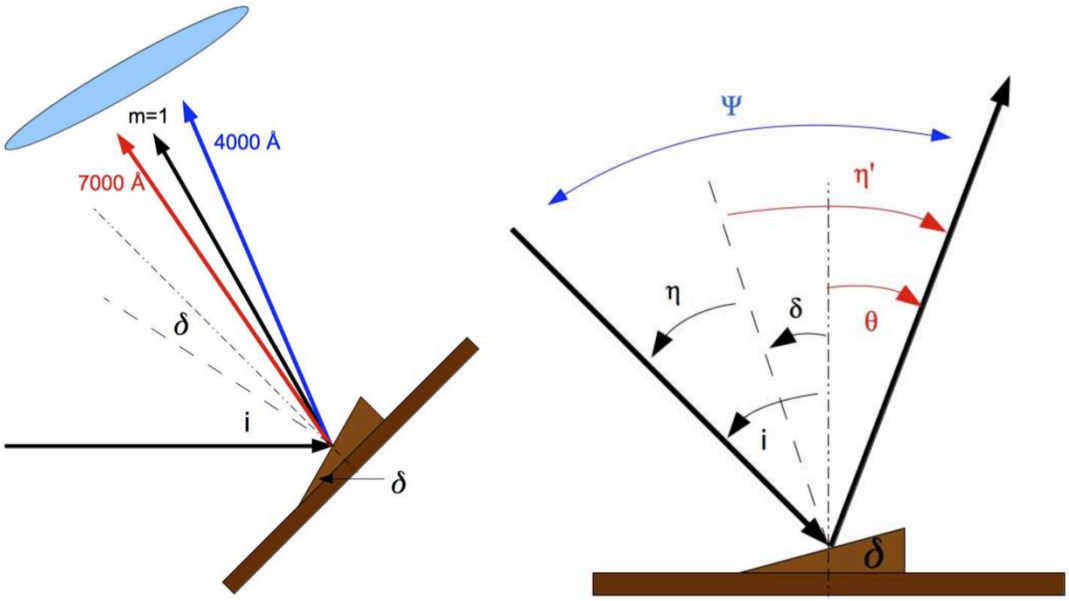

Figure 3 The Blaze angle δ: the maximum of intensity is moved to m=1. Right: chenage of the reference system to evaluate the maximum of the Blaze function.

In Figure **3** the distance between a line and the adjacent one is b=d*cos δ. For low order gratings δ is normally <10°, but it can reach a value around 60°-70°, for example in the echelle gratings.

The intensity of the light dispersed by a blazed grating follows the equation:

$$I = A_0^2 \frac{\sin^2 \beta}{\beta^2} \frac{\sin^2 (N\gamma)}{\sin^2 \gamma}$$

where:

$\frac{\sin^2 \beta}{\beta^2}$ is the Blaze Function and modulates the intensity of the interference function;

$2\gamma = \frac{2\pi}{\lambda} d \sin\vartheta = kd \sin\vartheta$ is the difference of phase between the centres of two adjacent lines;

$\beta = \frac{\pi}{\lambda} b \sin\vartheta = k \frac{b}{2} \sin\vartheta$ is the difference of phase between the centre and the side for each line.

Changing the reference system of the angles involved into the calculus as in Figure **3** (right), using the grating equation, we can find a new form for the Blaze function:

$$\beta = \pi b \rho m \left[\cos\delta - \frac{\sin\delta}{\tan\frac{i+\vartheta}{2}} \right]$$

This equation is not so easy to understand, but it is useful to find maximum and minimum values:

maximum value is for $\beta = 0 \Rightarrow i + \vartheta = 2\delta \Rightarrow \eta = -\eta' \Rightarrow i + \vartheta_b = 2\delta$

Applying this last condition to the grating equation $\sin i + \sin \vartheta_{blaze} = \rho m \lambda_{blaze}$ we can find the value of the so called Blaze wavelength:

$$\lambda_B = \frac{2 \sin \delta \cos(i - \delta)}{\rho m}$$

$$\lambda_B = \frac{2 \sin \delta \cos \frac{\psi}{2}}{\rho m}$$

where $\psi = i - \vartheta_{blaze}$ is the mechanical angle between the optical axis of the camera and the optical axis of the collimator (see Figure **3**, right panel).

1.4 Gratings

It has been shown the main features of the dispersing element, focusing on the geometrical properties. Moreover, the description is related to a spectrograph working at a single diffraction order (usually order +/-1). In this context, we have to consider if the grating works in transmission or reflection. The difference between the two is mainly related to the geometry of the spectrograph, which is considerably different in the two cases. In addition, the manufacturing tolerances are different as occur for lenses and mirrors and the grating working in transmission can be coupled with prism making the so called GRISM, which has a very nice feature of having the monochromatic image of the target at the same location as a direct image obtained with the GRISM removed. This approach is mostly suitable for low and medium dispersion spectrograph.

Another aspect to take into account when we consider the grating, consists in the fact that some technologies are more suitable for making transmission gratings than reflection gratings. Among the different possibilities we can focus on three:

- Ruled Blazed Gratings;
- Volume Phase Holographic Gratings;
- Lithographic Gratings.

The **Ruled Blazed Gratings** are the classical gratings with grooves characterized a certain period and angle as already explained in this document. We have to consider the fact that they are usually copies of master gratings and the manufacturing of a master one in extremely time consuming and expensive. The quality of the copies is variable and the size of the grating is usually limited. Moreover, it suffer of a efficiency reduction when the line density increase (high dispersion) and the presence of ghosts due to the ruling process (Rowling ghosts).

Volume Phase Holographic Gratings are the reference dispersing element for modern astronomical spectrographs. They are characterized by a periodic modulation of the refractive index induced in a thin layer of a suitable holographic material. The layer in embedded in between two glass substrates, so it is easy to apply high efficient AR

coatings. Moreover, the VPHG works very well in a GRISM configuration. The size of the VPHGs depend on the writing set-up and the actual limit is 300 mm perpendicular to the dispersion direction and the double in the dispersion direction (a mosaic approach is possible with a decrease of the overall efficiency).

The diffraction efficiency is another key aspect of this technology. Indeed, the peak efficiency can reach 100% (also at very high dispersion) and it can be tuned in wavelength just by changing the incidence angle. In figure XX, the typical diffraction efficiency curves as function of the incidence angle:

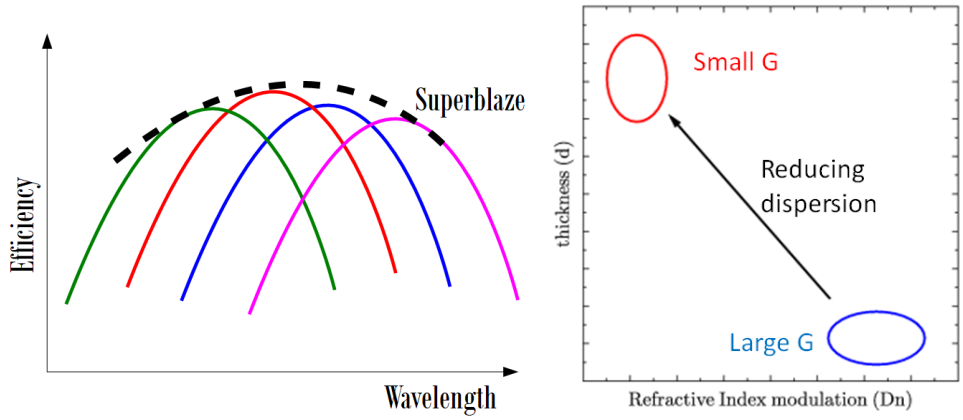

Figure X. On the left: Sketch of the diffraction efficiency curves for a VPHG as function of the incidence angle. On the right: the general scheme of the two parameters that determine the efficiency of a VPHG.

The diffraction efficiency of a VPHG depends on:

- Film thickness (d);
- Refractive index modulation (Δn);
- Profile of Δn;
- Line density (G);
- Average refractive index of the medium.

According to the Kogelnik model (true for high dispersion gratings), a large peak diffraction efficiency is obtained if the Bragg condition is met, that means the incidence angle (α) and the diffraction angle (β) are equal (equivalent to the Littrow condition). Moreover, as a rule of thumb, the product of Δn and d must be close to half of the wavelength at which a peak efficiency is required:

$$d \cdot \Delta n \approx {}^{\lambda}/_{2}$$

The bandwidth (angular and spectral) of the diffraction efficiency curve follows the equations:

$$\Delta\alpha \propto \frac{1}{Gd}$$

$$\frac{\Delta\lambda}{\lambda} \propto \cot\frac{\alpha}{Gd}$$

It is therefore apparent that a large peak efficiency can be obtained playing with the two film parameters d and Δn, but in order to obtain a wide efficiency band, it is necessary to decrease the film thickness d especially for small pitch grating (large G). As a consequence, the Δn must increase to maintain a high peak efficiency.

Sometimes the gratings diffract the light with a non-negligible efficiency in more than one order and this occurs mainly at low dispersion. In this case, it is important to understand how much energy is diffracted in the orders larger than one (LP). An approximated relation is the following:

$$LP \propto \frac{1}{\rho^2}$$

where $\rho = \lambda^2 G^2 / n\Delta n$.

The common range for the two parameters is: d = 3 – 30 μm, Δn = 0.001 – 0.11.

Lithographic Gratings are innovative devices that are becoming interesting also in the astronomical field. They usually show a binary profile characterized by a thickness (d) and a duty cycle (g/b):

Figure X. Scheme of a lithographic binary grating.

They can be produced using a laser/ebeam lithography approach or by using the holographic approach. At the moment, using the lithography the largest sizes are similar to those of VPHGs. By means of holographic approach, 700 mm in diameter can be achieved (monolithic in silica) and 1000 mm in diameter (silica coated).

An interesting feature of such lithographic grating is the large diffraction efficiency especially at high dispersion and in the visible. Indeed, this turns into a small size of the periodic structure and a small thickness. The efficiency can be also tuned by filling the pattern with a material with different refractive index.

According to the status of the technology, we can summarize the grating element and choice as function of the dispersion as follow:

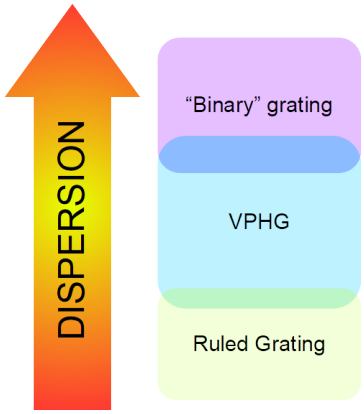

Figure X. Scheme of the choice of the grating technology as function of the required dispersion in the spectrograph.

Cleary, other aspects have to be considered (cost, production time and reliability). Moreover, we do not have consider the echelle approach that exploit a coarse grating at high diffraction orders. In this way, very high resolution can be achieved in an over-octave spectral range, but it is suitable for a single target (or a few).

1.5 spectrographs: the slicer.

In order to feed the spectrograph with light from the telescopes, and to reduce the effect of image motion causing variations in the slit illumination and corresponding variations in the spectral line shape which would mask the tiny radial velocity changes we are trying to measure, optical fibers are used to feed the light. Main disadvantage to this are:

1) the fiber can introduce modal noise. Many are the strategies to mitigate this problem, normally present in infrared spectrographs: octagonal fibers, photonic lanterns, mechanical scrambling, the use of an active or passive system to increase the uniformity if the illumination in the input termination of the fiber and others.

2) focal ratio degradation: the output of the fiber is wider (lower f/ratio) than the fiber input which decreases the spectrograph resolution.

In order to combat these effects and increase the resolution, which is needed to measure the tiny 1/1000th pixel shifts caused by low mass planets, image slicers are typically used to reformat the output fiber into a new more slit-like shape. The classic example is the Bowen-Walraven image slicer which uses a glass plate and prisms to slice the circular fiber image into two or more semi-circles and stack them on top of each other. Higher efficiency versions using mirrors or glass slabs have been made more recently.

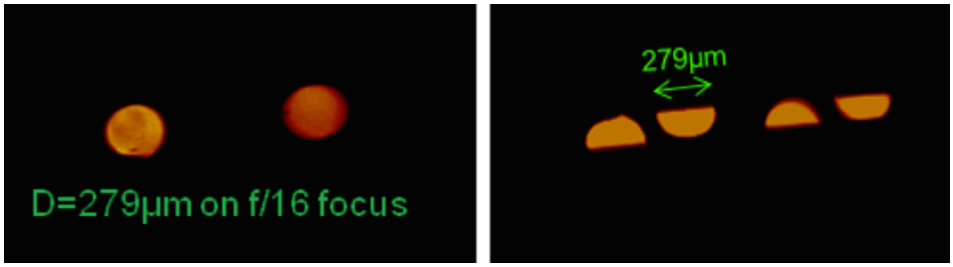

Figure 4 Example of a classical image slicer based on Bowen-Walraven prism (Giano-TNG spectrograph, first light prelist system)

Using a fiber fed spectrograph it is possible to increase the number of slice reassembling the position of the terminations of a fiber bundle, as visible in Figure 5.

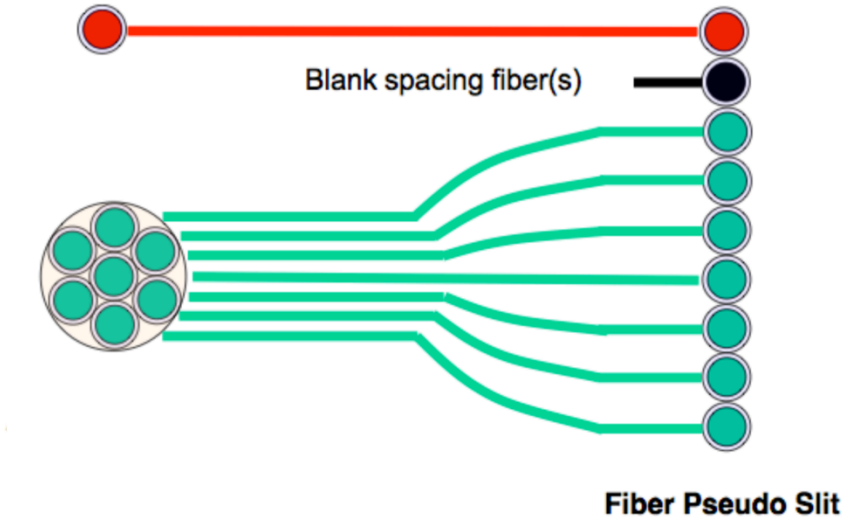

Figure 5 The fiber bundle output termination is arranged a Pseudo Slit shape

It is convenient to use a squared geometrical shape for the fibre input terminations let say a matrix of 3X3 or 4x4 fibers. The number of the fibers is directly connected to the Pseudo Slit length:

$$W_{long\ slit} = N \cdot D_{buffer}$$

where N is the number of fibers (for a 4x4 rectangular bundle N=16) and D_{buffer} is the mechanical diameter of the fiber, that it is different from the core diameter of the fiber that transmits the light. Normally, for telecom fibers, we have D_{buffer}=125um, while the core can have a dimension form 8um to 110um.

Normally to have an appropriated data reduction the width of the slit has to be around three times the pixel dimension (PS= Pixel Sampling), while the dimension $l_{pix,}$ of the single pixel is 9-10 um for the E2V detector. Taking into account equation (1) we find that it is necessary to use a fiber core diameter around 60 um, that it means to use a fiber having a buffer diameter of around 65 (see fiber model XXXX).

Now we can calculate the possible number of objects:

If N_{pix} is the number of the pixels along one side of the detector (typical value is 10000, pixel size l_{pix}=9 um, CCD dimension 90x90 mm) we obtain:

$$N_{objects} = \frac{L_{CCD}}{D_{buffer}/D_{core}} \cdot \frac{1}{PS} \cdot \frac{1}{N}$$

For example:

$N_{objects}$=160 @ N=16 (slicer 4x4), PS=3 (typical pixel sampling), L_{ccd}=10mm, D_{buffer}/D_{core}=1.3 (for fiber model having D_{core} = 50um and D_{buffer}=65 um)

Values can be changed in the Excel HR-MOS Calculator (ExMoCa) in the Sheet “Slicer”.

These type slicer, based mainly on a mosaic, is able to realize a field slicing when it is placed on the focal plane of the telescope, but it can be used in the same configuration as “pupil slicer” if it placed at the end o a big fiber placed in the telecope focal plane.

In the following some possible solutions of different type of mosaic are shown, based on the OPTIMOS-EVE for E-ELT for a Mono-Object (MO), a type of medium-IFU (MI) and a type of large-IFU (LI)[1]

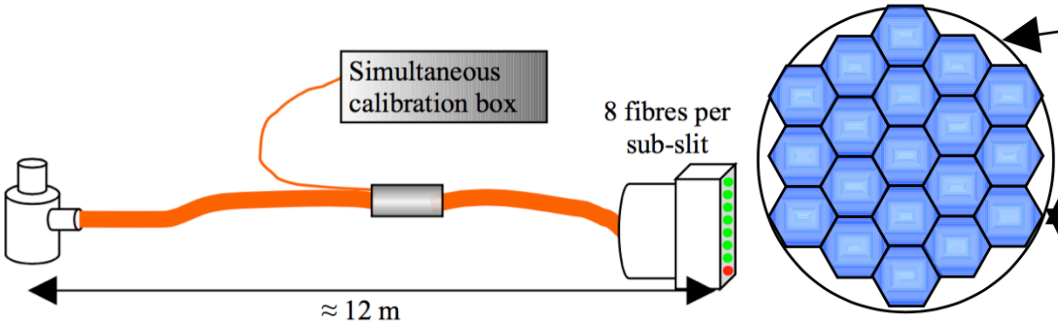

Figure 6 Mono-Object (MO), medium resolution layout configuration

The design of the MO-HR, see Figure **7**, is based on a buttons and is conceptually different from that of the MO-LR (see Figure **5**) and MO-MR sets. In the MO-HR button the circular input aperture on the sky, let say 0.8 arcsec, is fed into a 7-fold array of 0.27" microlenses. At the output of each subsequent fibre (core diameter 200 μm) a 7 microlens array of each 0.09" dividing the aperture into 7 subapertures. So the 0.81" input aperture is thus divided in 7x7= 49 sub-apertures of 0.09", to achieve the high resolution required. The diameter of these final fibres is 67 μm.

The reason why we have not chosen to put the 0.09'' microlenses directly in the focal plane like in other modes is that the focal length is shorter than the aperture diameter, making it impossible to fold the button with a 90° prism. Also, having a relay in the middle of fibre allows to increase scrambling in the fibre, and thus to improve radial velocity accuracy with a more homogeneous flux at 0.09'' fibre output.

[1] "*Development of five multifibre links for the OPTIMOS-EVE study for the E-ELT*", Isabelle Guinouard, Fanny Chemla, Hector Flores, Jean-Michel Huet, François Hammer, Gerben Wulterkens, arXiv:1009.1816v1, 10.1117/12.856232

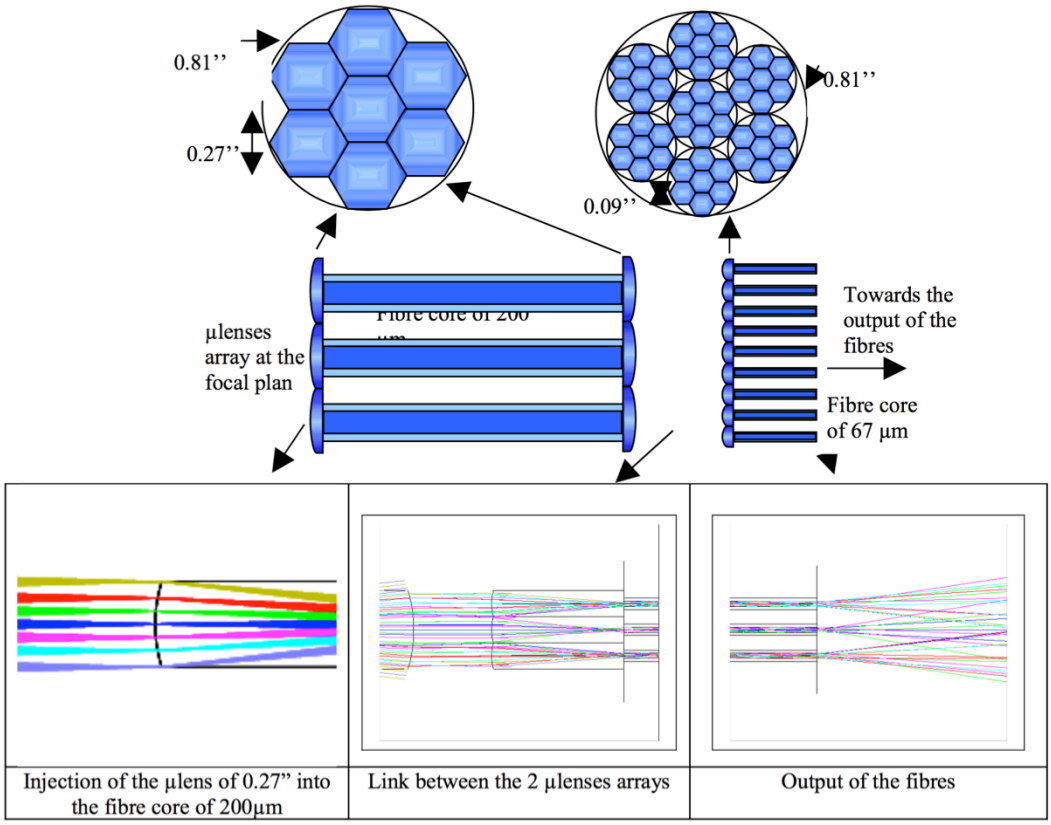

Figure 7 Mono-Object (MO), High Resolution

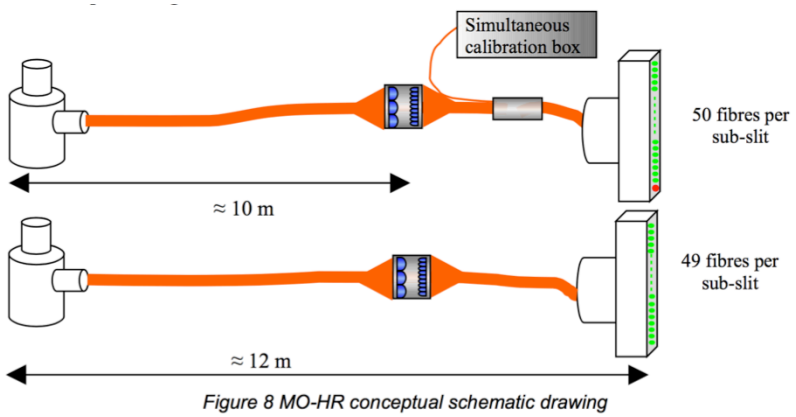

Figure 8 MO-HR conceptual schematic drawing

Figure 8 MO-HR conceptual design and IFU schema

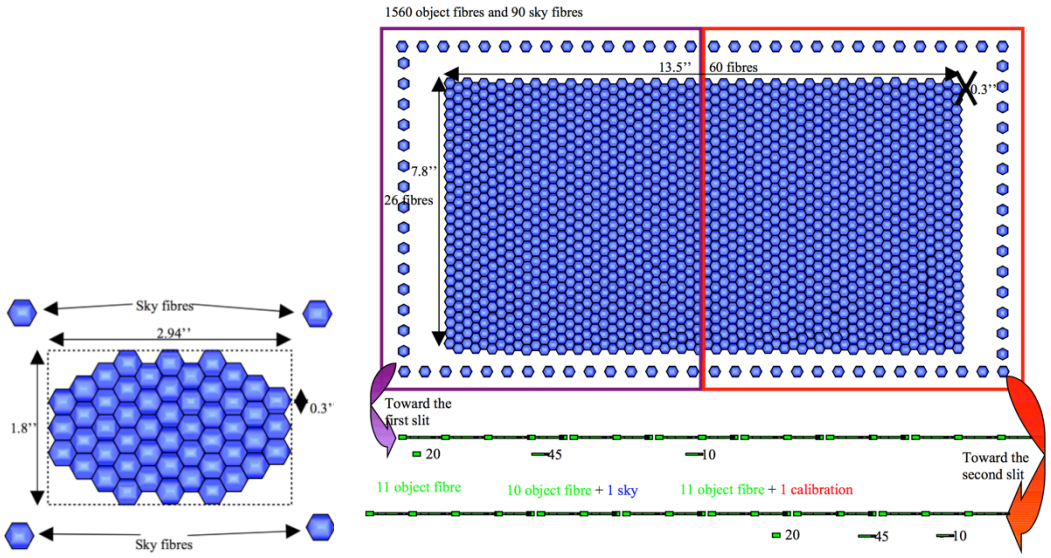

Figure 9 Medium-IFU Low Res (left). Large-IFU Low Res (right)

1.6 Spectrographs: the design

One of the possible solutions for the optical design of the spectrograph is the one based on HERMES, as visible in Figure **10**. The pseudo slit is placed in the focal plane of the collimator mirror and the use of a corrector lens is necessary to compensate the off axis configuration. The terminations of the fibers are placed on a curved surface to adjust the single chief ray of each fiber in the right geometry to have the pupil position located as near as possible on the dispersers: this mainly to reduce the dimension of these so expensive and challenging optical devices. The mechanical dimensions and the geometrical configuration of this solution implies that the pupil position is placed far from the collimator and the use of one or more than one folding mirror is necessary to have the curvature of the pseudo slit in the same geometry for each of the fours detectors. This fact has been noticed for example in MOONS-ESO spectrograph and coherently the solution used is a three arms placed in the same side.

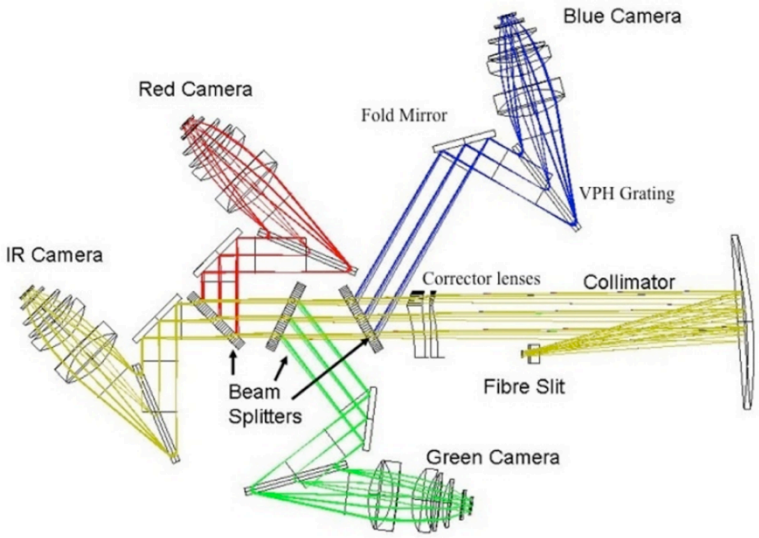

Figure 10 HERMES optical design schema